

PREDICTING THE OPTIMUM AIR PERMEABILITY OF A STOCK OF DETACHED ENGLISH DWELLINGS

Benjamin Jones^{*1}, Robert Lowe²

*1 Department of Architecture and Built Environment
Lenton Firs House, University of Nottingham
NG7 2RD, United Kingdom
*Corresponding author:
benjamin.jones@nottingham.ac.uk*

*2 Energy Institute
University College London
Central House, 14 Upper Woburn Place
London, WC1H 0NN, United Kingdom*

ABSTRACT

Mechanical positive input and extract ventilation are common strategies employed in English houses, generally because they provide adequate indoor air quality and specifically because they are effective at minimizing mould growth and its associated negative health consequences. Air is either exclusively supplied or extracted (never both) by a mechanical system at a prescribed airflow rate designed to ensure adequate indoor air quality. The remaining airflow, required to balance mass through the building, occurs through the fabric, through a mix of purpose provided and adventitious airflow paths. However, there is an important need to reduce adventitious airflow during the heating season in order to save energy and this is highlighted by the building standards of many countries who advocate increasing the airtightness of their housing stocks. Increasing a fabric's airtightness also increases its resistance to airflow and so a positive displacement or extract ventilation system must balance the corresponding increase in the fan power required to overcome this resistance with the need to provide an adequate supply of fresh air. Accordingly, the total energy consumption attributable to these ventilation systems during the heating season is a function of the dwelling's infiltration rate and heating system efficiency, and the fan's hydraulic power and efficiency.

This paper explores the possibility of an optimum air permeability for detached (single family) English houses ventilated by a mechanical positive input or an extract ventilation strategy. Firstly a theoretical model of air infiltration and exfiltration is used to investigate the underlying relationship between the fabric airflow rate, the mechanical ventilation rate (supplied or extracted), and the air permeability in a single detached dwelling. A meta-model of the total ventilation rate and heating system energy demand is developed. Secondly, the infiltration model then utilises a sample of over 16,000 English houses located in 10 different regions to investigate the relationship between the fan power and air permeability in a randomly chosen sub-sample of detached English houses. Thirdly, it is shown that there is indeed an optimum permeability for detached English houses with such systems and the effects of heating system and fan efficiencies on this value are identified. Finally, these predictions are contextualised by exploring their relevance to the current English housing stock.

KEYWORDS

Ventilation, infiltration, mechanical, positive-input, DOMVENT

1 INTRODUCTION

Mechanical ventilation systems are found in many European dwellings, particularly in the kitchen and bathroom where they are used maintain adequate indoor air quality (IAQ). A mechanical extract ventilation (MEV) fans reduce the internal air pressure below ambient and causes fresh air to be drawn through openings (commonly adventitious air leakage paths (ALPs) (Stephen, 2000)) in the thermal envelope. Positive input ventilation (PIV) reverses this process by supplying a steady flow of fresh air through a single opening located at the top of a stairwell.

The need to save energy is highlighted by the building codes of many countries that advocate increasing the airtightness of their housing stocks to save energy by reducing adventitious infiltration and exfiltration during the heating season. However, increasing the airtightness of a dwelling's fabric increases its resistance to airflow and when using a continuous CMEV (CMEV) or PIV system one must balance the corresponding increase in the fan power required to overcome this fabric resistance with the consequent reduction in spatial and temporal variation in air flow (Lowe, 2000). Accordingly, the total energy consumption

attributable to these ventilation systems during the heating season is a function of the dwelling's permeability, the heating system efficiency, and the fan's specific power.

An understanding of the interaction between CMEV and PIV, and infiltration and exfiltration is critical to the optimization of their performance and the minimization of energy consumption. Accordingly, this paper uses a theoretical approach to explore these relationships and asks the question: is there an optimum permeability for English houses ventilated using a CMEV or PIV system?

2 A MODEL OF VENTILATION AND ASSOCIATED HEAT LOSS

This paper applies DOMVENT3D, a model of infiltration and exfiltration through any number of façades that incorporates a mechanical ventilation system. The model was conceived by Lyberg (2000), initially developed and applied by Lowe (2000) and extended significantly by Jones *et al.* (2013a, 2014). Its assumptions, merits, limitations, and the corroboration of its predictions are discussed widely by Jones *et al.* (2013a, 2014), and an analysis of the sensitivity of its predictions to its inputs is undertaken by Jones *et al.* (2013b). The model, which is implemented using bespoke MATLAB (MathWorks, 2013) code, is discussed in Section 2.1. It requires inputs that may be unique to each dwelling or are general to a geographic region. Unique inputs comprise dwelling geometry, the flow exponent, internal air density, scaled wind speed, and façade wind pressure coefficients. General inputs are the ambient air temperature, regional wind speed, and wind orientation. Sources of data are discussed in Section 2.2.

2.1 Model of Ventilation and Associated Heat Losses

DOMVENT3D makes two assumptions about a façade: (i) it is uniformly porous; (ii) the pressure distribution over it is linear. It integrates the airflow rate in the vertical plane to predict the total airflow rate Q_i (m^3/s) through the i^{th} of j façades (Jones *et al.*, 2014) where

$$Q_i = \alpha(|\Delta p|/\Delta p) \int_{z_{min}}^{z_{max}} (|\Delta p|)^{\beta} dz \quad (1)$$

Here, z_{max} and z_{min} are the upper and lower height of a façade, Δp (Pa) is the pressure difference across an infinitesimal section dz (m) of a façade in the vertical plane, and α ($\text{Pa}^{-\beta}$) is a flow coefficient. Jones *et al.* (2014) show that $\alpha = E(2\bar{\rho})^{0.5} W$, where E is a dimensionless relative leakage area calculated from a known value of air permeability Q_{50} ($\text{m}^3/\text{h}/\text{m}^2$) or an equivalent metric, $\bar{\rho}$ (kg/m^3) is the mean of the internal and external air densities, and W (m) is the façade width. The net airflow through all j façades is zero

$$\sum_{i=1}^j Q_i + Q_M = 0 \quad (2)$$

where Q_M (m^3/s) is the airflow through a mechanical system and the positive sign indicates airflow into a building. An important feature of the model that makes it suitable for this study is its dynamic neutral height z_0 (m) which is described by

$$z_0 = \frac{\frac{1}{2}\rho_E u^2 c_p - p}{(\rho_{ext} - \rho_{int})g}. \quad (3)$$

Here, ρ is the air density (kg/m^3), u is the wind speed at building height (m/s), c_p is a mean façade wind pressure coefficient, g is the gravitational acceleration (m/s^2), p (Pa) is the internal air pressure (gauge), and the subscripts *int* and *ext* represent internal and external conditions, respectively. DOMVENT3D makes two further assumptions about the dwelling: (i) all rooms are interconnected and internal flow resistances are small so that a dwelling can be treated as a single-zone (Jones *et al.*, 2013a); (ii) each horizontal and vertical surface of the external envelope requires only a single flow equation linked by a continuity equation; Once the total ventilation rate at an instant in time $Q_I(t)$ (m^3/s) is predicted by DOMVENT 3D, the ventilation heat loss (W) is calculated by

$$H(t) = Q_I(t)\bar{\rho}c\Delta T(t)|_{T_{ext} \leq (T_{int}-3)} \quad (4)$$

where c is the specific heat capacity of air ($\text{J kg}^{-1}\text{K}^{-1}$), $\bar{\rho}$ is the mean of ρ_{ext} and ρ_{int} , and ΔT is the difference between the internal and ambient air temperatures. The internal air temperature, T_{int} ($^{\circ}\text{C}$), of an average unheated English house is, on average, 3°C higher than the ambient air temperature, T_{ext} ($^{\circ}\text{C}$), and so the heating system is assumed to function only when the ambient air temperature is $T_{ext} \leq 3^{\circ}\text{C}$ below the internal air temperature (Hamilton *et al.*, 2011). Heat loss is only calculated when the heating system is “on” and so Equation (4) is integrated over the entire heating season to estimate the total energy required by a heating system, H_I (MWh). Further energy may be required by a fan whose hydraulic power $\mathcal{P}_M = |p\dot{Q}_M|$ (W) is also integrated over the heating season to estimate the total fan energy demand, H_M (MWh). The total energy demand H_T (MWh) is given by $H_T = H_I/\mu_H + H_M/\mu_M$, where μ_H and μ_M are the heating system and fan efficiencies, respectively.

3 SOURCES OF DATA

The model is now used to predict the total heat lost from a typical detached (single family) dwelling located in an urban area of London and to investigate the underlying relationships between a CMEV or PIV system and adventitious airflow. The dwelling’s geometry, physical, and environmental properties are largely obtained from the 2009 English Housing Survey (EHS) (DCLG, 2011), a statistically representative sample of 16,150 dwellings that represents the 22.3 million dwellings of the English Housing stock. The sources of data are documented by Jones *et al.* (2013a) and so are only briefly discussed here.

Data inputs to DOMVENT3D may be divided into three distinct types: geometric, physical, and environmental. We now discuss each data type in turn beginning with geometric data. The EHS assumes that two connecting cuboids can reasonably represent the geometry of ~98% of English dwellings. The cuboid model applied here directly follows the Cambridge Housing Model (CHM) (Hughes *et al.*, 2012) used to estimate energy use and CO₂ emissions in the English stock for the UK government. For each façade the model requires the parameters z_{max} , z_{min} , and W . Dwelling orientation is not given by the EHS and so it is assumed to be a uniformly distributed random variable between 0 and 359 degrees ($^{\circ}$).

DOMVENT3D requires three key physical parameters: Q_{50} , dwelling β , and façade c_p . The former is varied between limits of 0.1 and $20\text{m}^3/\text{h}/\text{m}^2$ in order to evaluate its effect on Q_T and H_T ; see Sections 4 and 5. The flow exponent variable characterises the airflow regime through an ALP and is a function of its geometry and surface roughness. Its value affects both the pressure difference across an ALP and the airflow rate through it. Sherman & Dickerhoff (1998) show that a mean value of $\mu=0.65$ with a standard deviation of $\sigma=0.08$ best represents more than 1900 measurements made in U.S. dwellings. This distribution is similar to the smaller international AIVC data set (Orme *et al.*, 1998) and so is applied with confidence as a Gaussian random variable. Wind pressure coefficients (c_p) are defined for the horizontal and vertical surfaces. For the latter, the algorithm of Swami and Chandra (1987) gives a normalized average wind pressure coefficient for long-walled low-rise dwellings and is a function of the angle of incidence of the wind, and local sheltering. The coefficient is then scaled to account for local shielding. Horizontal surfaces are assumed to be completely shielded from the effects of the wind following Sherman and Grimsrud (1980).

DOMVENT3D requires seven key environmental parameters: geographic location, local wind speed and direction, T_{int} and T_{ext} , terrain type, and shielding. The EHS indicates the region in which each sample is located and allows suitable weather data to be chosen from the CIBSE Test Reference Year (TRY) weather data set (CIBSE, 2002). This source provides synthesised typical weather years for 10 English regions and is suitable for analysing the environmental performance of buildings. Accordingly, each EHS region is mapped to an appropriate CIBSE TRY region and where more than one CIBSE region is located in an EHS region the CIBSE region is chosen randomly (with equal probability) from the set of possible regions. The TRY weather data provides local wind speed, wind direction, and T_{ext} at hourly intervals. The wind

speed is scaled according to the terrain and dwelling height using a standard power law formula (BSI, 1991). Dwelling height is obtained from the cuboid model and the terrain type is indicated by the EHS. The four BSI terrain types and the local wind pressure shielding coefficients of Deru and Burns (2002) are mapped to the six EHS terrain types with format EHS (BSI){Deru and Burns}: city (city){very heavy}, urban (urban){heavy}, suburban town (urban){heavy}, rural residential (urban){moderate}, village centre (urban){moderate}, rural (country with scattered wind breaks){light}. Finally, DOMVENT3D is not a thermal model and so T_{int} must be prescribed. Here, a gaussian distribution of thermostat temperatures is chosen with $\mu=21.1^\circ\text{C}$ and $\sigma=2.5^\circ\text{C}$ following Shipworth et al. (2009) who calculate these values from measurements made in a representative sample of 196 English dwellings.

4 PREDICTING VENTILATION ENERGY DEMAN OF A SINGLE DWELLING

The model is now used to investigate the underlying relationships between the CMEV and PIV systems and adventitious airflow using a detached (single family) dwelling located in an urban area of London. The dwelling is selected at random from the EHS database and its geometry, physical, and environmental properties and are given in Table 1. Their sources are described in Section 3, but for random variables, such as orientation, β , and T_{int} , typical values are chosen, where possible, for illustrative purposes. The fan provides an normalized (by dwelling volume) airflow rate of $N_M = \pm 0.5\text{h}^{-1}$, which is recognised by many European countries as a threshold ventilation rate below which some negative health effects increase (Jones *et al.*, 2013a). The sign indicates the flow direction, which is dependent on the mechanical system. Both CMEV and PIV systems are investigated and predictions of heating season ventilation air change rate and ventilation heat loss (excluded fan energy use) with varying Q_{50} are given in Figure 1 and compared against those for naturally occurring infiltration and exfiltration (with no mechanical system). Here we note two things. Firstly, the predictions of heating season ventilation rate made with and without a mechanical system are both described by the terms N_I or Q_I , where the former term is a normalized version of the latter using dwelling volume, but for clarity and brevity we use the subscript NV to describe the airflow solely attributable to natural airflow forces when $Q_M = 0$, and the subscript T to describe airflow where a mechanical system is present when $Q_M > 0$. Secondly, the terms Q_{50} and N_{50} (the air change rate at a pressure differential of 50Pa) can be considered almost identical because the sample dwelling's surface area to volume ratio is approximately unity; see Table 1.

Figure 1 shows that N_{NV} and its corresponding heat loss increase linearly with Q_{50} . Ventilation rates for CMEV and PIV are similar, differing by $\sim 2\%$ at $20\text{ m}^3/\text{h}/\text{m}^2$. At the limits of Q_{50} . As $Q_{50} \rightarrow 0\text{ m}^3/\text{h}/\text{m}^2$ the ventilation rate is $N_T \approx N_M$, and the ventilation heat loss $H_I \propto N_M$. These relationships are explained by considering Figure 2, which gives the variation of z'_0 , the mean dimensionless relative neutral height (relative to the dwelling height) for all façades during the heating season, with Q_{50} . It shows that $|z'_0| < 1$ when $Q_{50} \lesssim 6\text{ m}^3/\text{h}/\text{m}^2$ indicating that, depending on the sign of Q_m , z_0 is either above the building ($z_0 > z_{max}$) or below the base of the building ($z_0 < z_{min}$) for most of the heating season. In these circumstances, the mechanical airflow rate is balanced by infiltration or exfiltration over the whole envelope. The location of z_0 is a function of p and so by rearranging Equation (3) it is possible to identify the environmental conditions when $z_0 > z_{max}$ or $z_0 < z_{min}$. Here, Equation (3) shows that a CMEV system raises $z_0 > z_{max}$ on any façade when $p < \left[\frac{1}{2} \rho_E u^2 c_p - (\rho_{ext} - \rho_{int}) g z_{max} \right]$. For the rare situation where $T_{ext} = T_{int}$ and $(\rho_{ext} - \rho_{int}) = 0$, the pressure difference across a façade does not vary with height, but the inequality still applies. Instead it describes the p required to overcome the prevailing environmental conditions and reverse the airflow direction through an entire leeward façade (when $c_p < 0$) so that air flows into a building. For the inequality to be true for a specific façade, either the

$u^2 c_p$ term is small in magnitude or $p \ll 0$. The latter occurs in airtight dwellings; for example, in the sample detached dwelling, Figure 1 suggests this is when $Q_{50} < 6 \text{ m}^3/\text{h}/\text{m}^2$. Conversely, a PIV system lowers $z_0 < z_{min}$ when $p > \left[\frac{1}{2} \rho_E u^2 c_p - (\rho_{ext} - \rho_{int}) g z_{min} \right]$. When $(\rho_{ext} - \rho_{int}) = 0$, the inequality still applies and describes the p required to overcome the prevailing environmental conditions and reverse the airflow direction through a windward façade (when $c_p > 0$) so that air flows out of a building. For the inequality to be true, either the $u^2 c_p$ term is small in magnitude or $p \gg 0$. The latter also occurs in airtight dwellings, which for the sample detached dwelling Figure 1 shows is when $Q_{50} \approx 6 \text{ m}^3/\text{h}/\text{m}^2$. This value of Q_{50} is identified by Lowe (2000) as a *critical* air permeability because it is the point where the gradients of N_T and H_I for PIV and MEV systems increase. It is interesting to note that Lowe also predicts the critical N_{50} to be around 6 h^{-1} , which is equivalent to $Q_{50} \approx 6 \text{ m}^3/\text{h}/\text{m}^2$ when the surface area to volume ratio is unity, although it is likely to vary across a housing stock.

When $Q_{50} \rightarrow 20 \text{ m}^3/\text{h}/\text{m}^2$ the dwelling can be considered to be *leaky* because Figure 1 shows that the total ventilation rate with mechanical assistance through the dwelling is predicted to be significantly more than the mechanical ventilation rate, N_M . It is also clear from Figure 1 that the total ventilation rate with mechanical assistance is $N_T \approx N_{NV} + C$, where C is the change in the ventilation rate attributable to the mechanical system. In these circumstances a CMEV system with a small airflow rate is responsible for a slight increase in the z_0 of all façades (see Figure 2) and a concurrent increase in the infiltration rate increases by ΔQ_{inf} (m^3/s) and decrease in the exfiltration rate by ΔQ_{exf} (m^3/s). The ΔQ_{inf} and ΔQ_{exf} terms are equal in magnitude but opposite in sign and so the total change attributable to the mechanical system is $|Q_M| \approx 2\Delta Q_{inf}$, or $\Delta Q_{inf} \approx |Q_M|/2 \approx C$. The same proof applies to a leaky dwelling ventilated by a PIV system, where z_0 decreases in all façades and when $T_{ext} = T_{int}$, where the CMEV or PIV system amends the magnitude of p and so that ΔQ_{exf} and ΔQ_{inf} are similarly equal in magnitude but opposite in sign. Here we note that the change in the total heating season space heating ΔH_I (MWh) required to compensate for the increased airflow rate caused by the addition of a CMEV or PIV system can be described in the same way, and so in the limit of small mechanically induced airflows $\Delta H_I \propto Q_M/2$. A simple function that fits the simulated data over the whole range of air leakage is given by

$$N_T = \left\{ |N_M^n| + \left(N_{NV} + \frac{|N_M|}{2} \right)^n \right\}^{\frac{1}{n}} \quad (5)$$

where $n = 8$ gives a maximum absolute error (MAE) of 1% over the entire range of Q_{50} for a CMEV system, and $n = 7$ gives a MAE of 3% over the entire range of $0 < Q_{50} \leq 20$ for a PIV system, where the MAE is a measure of the largest deviation of the model's outputs. Figure 4 shows that the relationship between n and the MAE is for the sample detached dwelling is non-symmetric about a minimum MAE. However, when the value of n is greater than the location of the minimum MAE, the gradient is small and tends to an asymptote. Accordingly, if the most appropriate value of n is unknown, a high value should be selected so that $n \gg 20$. For the sample detached dwelling, $n = 20$ gives a MAE of $< 0.03 \text{ h}^{-1}$ or $< 5\%$ across the range of $0 < Q_{50} \leq 20$.

The model can be augmented by applying another simplified models that predicts N_{NV} from Q_{50} or N_{50} ; see Jones *et al.* (2013). Further work is required to investigate the suitability of Equation (5) for predicting N_T in English houses that accounts for the variance of the inputs to the DOMVENT3D model (see Section 3). This is undertaken in Section 5.

Figure 5 shows the total predicted fan energy demand during the heating season, H_M . There is little difference between the predictions for the CMEV and PIV systems, but Figure 5 shows that there is a minimum value that occurs in the region of the *critical* permeability, where

Table 1: Properties of sample detached dwelling.

EHS sample	G0322417
Dwelling type	Detached
Location	London, England
Terrain type	Urban
Sheltering	Heavy
Orientation	North/south
Height (m)	5.1
Width (m)	6.4
Depth (m)	7.2
Volume, V (m ³)	232.7
Surface area, A_{surf} (m ²)	229.5
$A_{surf}:V$ (m ² /m ³)	1.01
β	0.6
T_{int} (°C)	21.1

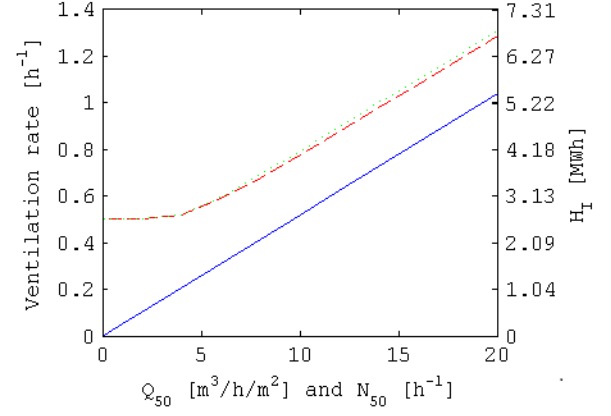


Figure 1: Predicted ventilation rate and heat loss, H_I (MWh), during the heating season.

—, natural infiltration; ---, CMEV; ···, PIV

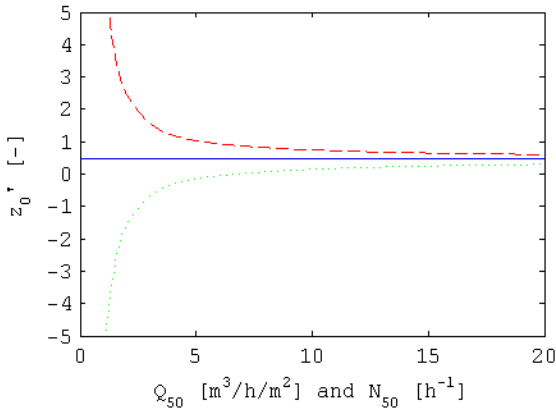


Figure 2: Predicted mean relative neutral height, z_0' , for all façades during the heating season.

—, natural infiltration; ---, CMEV; ···, PIV.

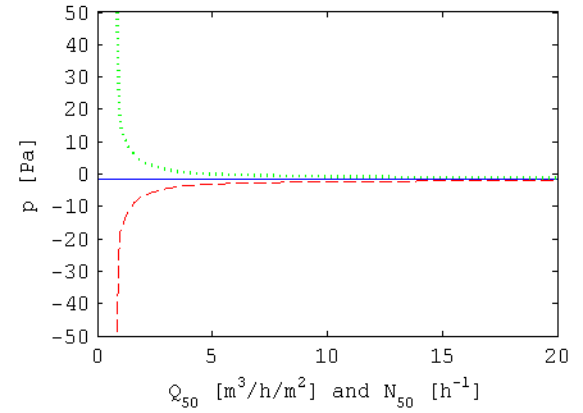


Figure 3: Predicted mean internal air pressure, p (Pa), for all façades during the heating season.

—, natural infiltration; ---, CMEV; ···, PIV.

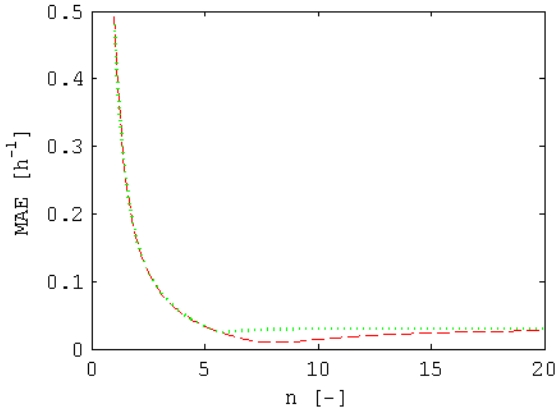


Figure 4: Change in maximum absolute error with n in English detached dwellings during the heating season. ---, CMEV; ···, PIV.

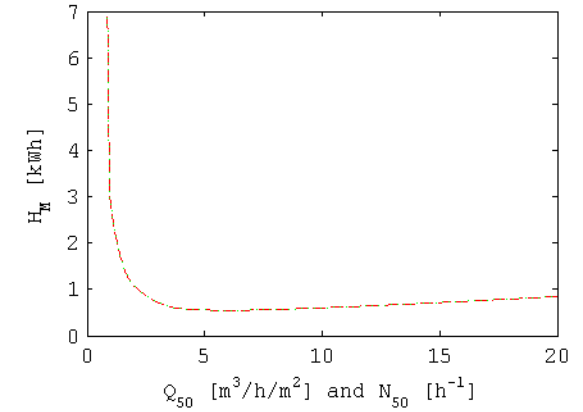


Figure 5: Predicted fan energy demand, H_M (kWh), during the heating season.

---, CMEV; ···, PIV.

$Q_{50} \approx 6 \text{ m}^3/\text{h}/\text{m}^2$. Section 2.1 shows that $H_M = f(N_T, p)$, whose respective relationships with Q_{50} are given in Figures 1 and 3. When $Q_{50} < 6 \text{ m}^3/\text{h}/\text{m}^2$ the internal pressure $|p| \rightarrow \infty$ as $Q_{50} \rightarrow 0$, and the airflow rate tends to an asymptote where $N_T \rightarrow N_M$. Accordingly, the air pressure p , strongly influences the hydraulic power because its gradient is steep. Conversely, when $Q_{50} > 6 \text{ m}^3/\text{h}/\text{m}^2$ Figure 3 shows that the internal pressure p , approaches a small asymptote and N_T increases linearly with Q_{50} . The airflow rate N_T , only has a moderate influence over the hydraulic power because its gradient is modest. Pressure losses within the

system are unaccounted for in this study because they are manufacturer-specific but it is possible they would increase the hydraulic power, particularly when Q_{50} is greater than its critical value. The application of multiple fans is also unaccounted for and, because their efficiencies may vary, they can reach a stalling point leading to an unstable airflow rate.

In Figure 7, H_M and H_I are summed to calculate H_T where the boiler and fan efficiencies are unity, $\mu_H = \mu_M = 1$. A minimum H_T is observed between $1 < Q_{50} < 2 \text{ m}^3/\text{h}/\text{m}^2$. A root finding technique that utilizes the Newton Raphson method (see Verbeke & Cools, 1995) finds the minimum or *optimum* permeability at $Q_{50} = 1.4 \text{ m}^3/\text{h}/\text{m}^2$ for both CMEV and PIV systems. Figure 6 shows the effect of systematically varying μ_M between 0.1 and 1, and μ_H between 0.1 and 4 (where $\mu_H > 1$ simulates the coefficient of performance of a heat pump) on the optimum permeability for a CMEV system. Figure 7 shows that the variation in the optimum permeability is non-linear and limited, increasing with μ_H and decreasing with μ_M . Although the performance of the heating and ventilation equipment is shown to influence the optimum permeability of a dwelling, it is likely that general and specific dwelling parameters (described in Section 3) affect the optimum permeability. Accordingly, this is investigated in Section 5.

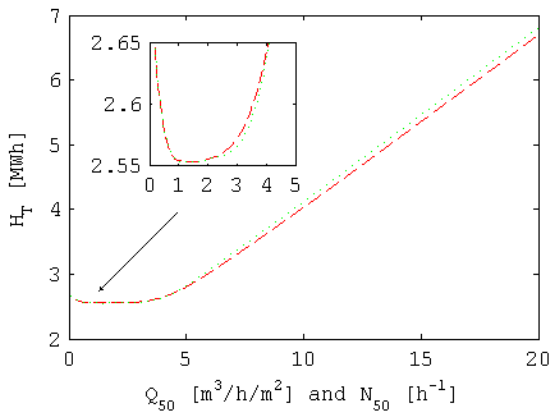


Figure 6: Predicted total energy demand, H_T (MWh), during the heating season.

---, CMEV; ···, PIV.

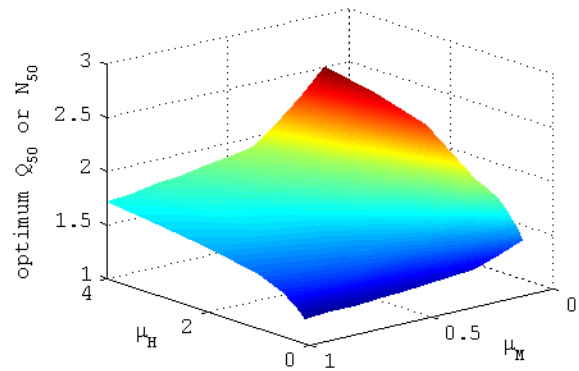


Figure 7: Optimum heating season Q_{50} and N_{50} with varying μ_H and μ_M for a CMEV system.

5 CONSIDERING STOCK VARIANCE IN ENERGY DEMAND

Section 4 considered the use of a CMEV or PIV in a single detached dwelling and identified a simple equation to predict the total ventilation rate from known mechanical and natural airflow rates; see Equation (5). However, it is desirable to know what the variance of the exponent n , is across the stock of English detached dwellings so that a general value can be identified. Section 4 shows that n differs according to the system employed and so both CMEV and PIV types are investigated using DOMVENT3D and a Monte Carlo (MC) sampling approach. There are four stochastic inputs to DOMVENT3D: the EHS sample (using dwelling weight), dwelling orientation, indoor air temperature, a flow exponent, and air permeability. A set of twenty samples of the 1st four inputs (hence excluding Q_{50}) are chosen at a time using a Latin Hypercube. However, the Q_{50} is varied systematically for each sample at values of 0.1, 2, 4, 6, 8, 10, 15, 20, and 50 $\text{m}^3/\text{h}/\text{m}^2$ (a total of 9 values). Accordingly, with a fan airflow rate of $N_M = \pm 0.5 \text{ h}^{-1}$ (see Section 4) nine predictions of N_T are made by DOMVENT3D for each sample to identify its relationship with Q_{50} ; see Figure 1. In addition, Figure 1 shows that the natural ventilation rate N_{NV} , during the heating season varies linearly with Q_{50} and so only a single prediction of N_{NV} is needed (apply the sample inputs used to estimate N_T) and is scaled by Q_{50} . The predictions of DOMVENT3D are then compared to those of Equation (5) for a range of exponents where $1 \leq n \leq 30$. The MAE for each value of n is used to identify the best n for each dwelling. The total sample size increases

incrementally according to the set size. After each set of predictions is made, the mean (μ) and standard deviation (σ) of n for the whole sample are calculated and used to decide if a stopping criterion has been met. The number of samples is deemed adequate if the change in μ and σ from one set of 20 samples to the next is less than 0.2% after a minimum of 5 sets (100 samples) have been obtained. The model is run twice because a distribution is required for each mechanical system.

Figure 8 gives distributions of n (see Equation (5)) for CMEV and PIV systems estimated using MATLAB's `ksdensity` kernel smoothing function (with a moderated bandwidth of 1.6 for the PIV system). The CMEV sample required 27 sets (540 samples) to converge, whereas the PIV sample required 11 sets (220 samples). Here, the mean and standard deviation of n for a PIV system are $\mu=4.5$ and $\sigma=1.5$, and the mode value is approximately equal to the mean value. A two-sample Kolmogorov-Smirnov (KS) test is used to test the null hypothesis that the data given in Figure 8 for a PIV system is Gaussian (with $\mu=4.5$ and $\sigma=1.5$) is rejected at a 5% significance level ($p=1.09\times 10^{-4}$). Accordingly, the mean value of $n=5.1$ is more appropriate for this stock of detached dwellings. The need for simplicity and brevity often necessitates the use of whole numbers, rather than fractions. Accordingly, Figure 8 suggests that an exponent of $n=5$ is broadly appropriate for detached English dwellings. Applying $n=5$ to the sample dwelling discussed in Section 4 gives a MAE of 0.03h^{-1} or 6% within the limits of $0.1 \leq Q_{50} \leq 20$.

Figure 8 shows that the distribution of n for a CMEV system is tri-modal, although it is clear that the majority of the data is located where $n \approx 9$. Here, $\mu=15.6$, $\sigma=9.6$, and the median value is $n=11$. A two-sample Kolmogorov-Smirnov (KS) test rejects the null hypothesis (at 5% significance) that the distribution is Gaussian (with $\mu=15.6$ and $\sigma=9.6$) ($p=2.86\times 10^{-8}$). Applying a rounded value of $n=11$ to the sample dwelling discussed in Section 4 gives a MAE of 0.02h^{-1} or 3% within the limits of $0.1 \leq Q_{50} \leq 20$. Here note that Figure 3 shows the relationship between n and the MAE to be asymmetric and so if the most appropriate value of n is unknown, a high value should be selected. Figure 8 suggests that the value of n propose in Section 4 should be increased to $n \gg 30$ in order to minimize the MAE for the whole stock of English detached dwellings.

The sampling method described earlier in this Section is now applied to estimate the distribution of the optimum permeability across the English stock of detached dwellings, although some small amendments are required. Firstly, Figure 5 shows that the minimum is likely to occur at low Q_{50} and so it is varied using a root finding technique (see Section 4) that searches for the minimum value of H_T . In addition, the boiler and fan efficiencies are given typical values. Here, Lowe (2000) suggests that a boiler efficiency of 90% ($\mu_H = 0.9$) is appropriate for most UK houses because many now contain condensing gas-fired systems,

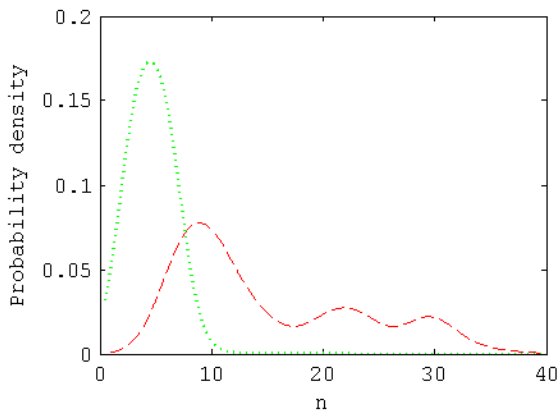


Figure 8: Distribution of exponent, n , in English detached dwellings during the heating season.

---, CMEV; ···, PIV.

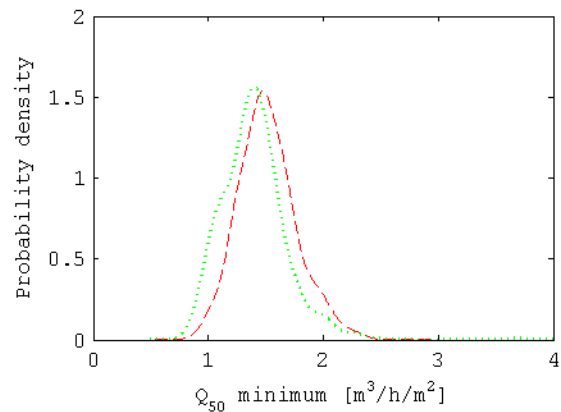


Figure 9: Distribution of optimum permeability in the English housing stock for the heating season.

---, CMEV; ···, PIV.

although extending the approach to other heating and electrical supply systems in the future would be trivial. CIBSE (2005) suggest that the total efficiency of an axial-flow fan (with or without guiding vanes) is approximately 65% ($\mu_M = 0.65$). The model is run twice because a distribution is required for each mechanical system.

Figure 9 shows predicted distributions of optimum Q_{50} in English detached dwellings during the heating season, when $\mu_H = 0.9$ and $\mu_M = 0.65$. The CMEV sample required 26 sets (520 samples) to converge, whereas the PIV sample required 24 sets (480 samples). The optimum permeability for CMEV and PIV are respectively found to occur at 1.5 and 1.4 m³/h/m², respectively, with most of the data lying between 1 and 2 m³/h/m². These airtightness values are considered to be very tight because they comprise <1% of UK dwellings built before 2000 (Stephen, 1998) and <2% of UK dwellings built after 2006 (Pan, 2010). Furthermore, Figure 3 shows that the required change in internal air pressure is up to 18 Pa, and so non-standard fan may be required. Lowe (2000) notes that the default system of an airtight dwelling is a balanced mechanical ventilation with heat recovery (MVHR), but shows that a badly designed, low-efficiency, system will always be outperformed by a CMEV system. This study confirms that there is merit in increasing the airtightness of dwellings that apply CMEV or PIV strategies to reduce ventilation heat loss. A demand control strategy could further reduce energy demand. Increasing fabric tightness is also important to ensure adequate IAQ because it is shown (Stephen, 2000) that a PIV system can force stale, warm, and moist air into the loft space where the moisture condenses and where it is recirculated back into the house reducing IAQ. A mechanical system can help to provide adequate indoor air quality in a dwelling and reduce the negative health consequences associated with under-ventilation. The increase in total energy demand that occurs at very low permeabilities is unlikely to be a problem in practice.

6 CONCLUSIONS

This paper utilises an existing model of infiltration and exfiltration and databases of dwelling geometry, dwellings' physical parameters, and environmental information to investigate the performance of mechanical extract ventilation and positive input ventilation systems in English detached houses during the heating season.

A sample detached house is used to investigate the underlying physics of the problem and finds that at low detached houses values of dwelling air permeability the total infiltration rate is approximately equal to the fan airflow rate. As the infiltration rate increases significantly, the total ventilation rate of the dwelling is approximately equal to the sum of the airflow rate found the same detached dwelling without a fan (naturally occurring infiltration and exfiltration) and half the fan's airflow rate. The same relationship applies to the demand placed on a heating system to replace lost warm air during the heating season. The relationship is described using a simple equation that includes an exponent. For the sample detached house the exponent is found to be different for the CMEV and PIV systems. Then, a stochastic method is used to predict distributions of the exponent for a stock of detached English dwellings. Their distributions show that geometric, physical, and environmental dwelling information does influence the most appropriate choice of exponent and a method that minimises the maximum absolute error is used to enable an appropriate value to be chosen for each of the CMEV and PIV systems. The model is of interest to policy makers of any country who use simplified energy models, such as the UK's standard assessment procedure, to make informed decisions.

When the energy demand of the mechanical demand ventilation system is considered in a sampled detached dwelling, an optimum air-permeability is found where the total energy demand is minimized. Then, a similar stochastic approach is used to investigate the location of the optimum air-permeability in the stock of English detached dwellings. It is found to occur at between 1 and 2 m³/h/m², which is only found in <1% of all UK dwellings

constructed before 2000. Accordingly, although theoretically possible, the reality of achieving an optimum permeability in a large number of houses ventilated by CMEV and PIV systems is unlikely. However, this highlights that the increase in total energy demand that occurs at very low air permeability is unlikely to be a problem in practice and that it is difficult to make a house too airtight.

7 REFERENCES

- CIBSE. (2002). Guide J - Weather, Solar and Illuminance data. London, CIBSE Publications.
- CIBSE. (2005). Guide B - Heating, Ventilating, and Air Conditioning. London, CIBSE.
- DCLG (2011). English Housing Survey: Headline report 2009-10. London, Department for Communities and Local Government.
- Deru, M.P. and Burns, P.J. (2003). Infiltration and natural ventilation model for whole building energy simulation of residential buildings. *ASHRAE Transactions* 109(2), 801-811.
- Hamilton, I., *et al.* (2011). The impact of housing energy efficiency improvements on reduced exposure to cold — the ‘temperature take back factor’. *BSER&T* 32(1), 85-98.
- Hughes, M., *et al.* . (2012). Converting English Housing Survey Data for Use in Energy Models, Cambridge Architectural Research Ltd. and University College London.
- Jones, B.M., *et al.* (2013a). The Effect of Party Wall Permeability on Estimations of Infiltration from Air Leakage. *International Journal of Ventilation* 12(1): 17-29.
- Jones, B.M., *et al.* (2013b). A stochastic approach to predicting the relationship between dwelling permeability and infiltration in English apartments. 34th Air Infiltration and Ventilation Centre, 3rd TightVent, 2nd Cool Roofs', and 1st Venticool Conference. Athens, Greece: 199-209.
- Jones, B.M., *et al.* (2014). Modelling uniformly porous façades to predict dwelling infiltration rates. *Building Services Engineering Research and Technology*. 35(4).
- Lowe, R.J. (2000). Ventilation strategy, energy use and CO₂ emissions in dwellings – a theoretical approach. *Building Services Engineering Research and Technology* 21(3), 179-185.
- Lyberg, M. (1997). Basic air infiltration. *Building and Environment* 32(2), 95-100.
- MathWorks (2013). MATLAB Version 8.3.0.532 (R2014a). The MathWorks Inc.
- Orme, M., Liddament, M.W. and Wilson, A. (1998). TN 44: Numerical Data for Air Infiltration and Natural Ventilation Calculations, Air Infiltration and Ventilation Centre.
- Pan, W. (2010). Relationships between air-tightness and its influencing factors of post-2006 new-build dwellings in the UK. *Building and Environment* 45(11), 2387-2399.
- Sherman, M.H. and Dickerhoff, D.J. (1998). Airtightness of U.S. dwellings. *ASHRAE Transactions* 104(4), 1359-1367.
- Sherman, M.H. and Grimsrud, D.T. (1980). Infiltration–pressurization correlation: simplified physical modelling. Lawrence Berkeley Laboratory Report LBL-10163.
- Shipworth, M., *et al.* (2009). Central heating thermostat settings and timing: building demographics. *Building Research & Information* 38(1): 50-69.
- Stephen, R.K. (2000). IP 12/00: Positive Input Ventilation in Dwellings. BRE, Watford, UK.
- Stephen, R.K. (1998). Airtightness in UK dwellings: BRE's test results and their significance, Building Research Establishment.
- Swami, M. and Chandra, S. (1987). Procedures for Calculating Natural Ventilation Airflow Rates in Buildings, ASHRAE.
- Verbeke, J. and Cools, R. (1995). The Newton-Raphson method. *International Journal of Mathematical Education in Science and Technology* 26(2): 177-193.